



Cite this: *Energy Adv.*, 2023, 2, 1521

## Dopant-free small-molecule hole-transport material for low-cost and stable perovskite solar cells†

Sahar Majidi-Nezhad,<sup>a</sup> Negin Sabahi,<sup>a</sup> Hashem Shahroosvand,<sup>a</sup> Narges Yaghoobi Nia<sup>bc</sup> and Aldo Di Carlo<sup>a</sup>

Dopant-free hole-transporting materials (HTMs) aim to improve efficiency and stability simultaneously, and are a promising direction for efficient perovskite solar cells (PSCs). To achieve dopant-free and low-cost HTMs, small organic molecules based on imidazole phenanthrene derivatives were easily prepared in a one-pot cycling reaction without the use of a catalyst or harsh conditions. The total cost of 1 g of this new HTM is about \$5, which is 1/20th of the cost of the benchmark HTM spiro-OMeTAD (>\$100). In particular, the power conversion efficiency (PCE) of PSCs based on the new HTM without using LiTFSI/4-*tert*-butylpyridine dopants is about 9.11%, which is higher than for PSCs based on spiro-OMeTAD, for which the PCE is 6.21% under the same conditions. Moreover, the light stability of PSCs based on the new additive-free HTM indicated good behaviour over 500 hours, resulting in only 10% loss of initial efficiency. The doped PSC also shows 14% efficiency, maintaining more than 80% of its initial efficiency after 500 hours of light exposure. The exclusive photovoltaic properties of the new HTM can be attributed to its high conductivity and hole mobility, which are related to the small size of the molecules compared to common HTMs known so far. These new HTMs represent a breakthrough in the engineering of additive-free PSCs based on organic HTMs, which will open up new avenues to achieve low-cost and high-stability PSCs.

Received 1st August 2023,  
Accepted 9th August 2023

DOI: 10.1039/d3ya00367a

rsc.li/energy-advances

## 1. Introduction

Following the COVID-19 crisis, the quest to replace fossil fuel energy with renewable and sustainable energy is an active field of research and a continuing problem.<sup>1</sup> As the most promising candidate amongst the latest developments in solar energy, perovskite solar cells (PSCs) have successfully passed a large number of criteria from various consortia aimed at promoting low-cost PSCs into the marketplace.<sup>2–4</sup> Their relatively low-cost abilities are due to the facile synthesis, tweaking, and tailoring of crystalline perovskite light absorbers, which are at the heart of the conversion of solar energy to electricity.<sup>5–7</sup> The flexibility of PSCs and their thin-film abilities facilitate large-scale

manufacturing processing techniques, such as inkjet printing, spraying,<sup>8,9</sup> and zero-waste scalable blade spin-coating. However, what has surprised the photovoltaic community has been the dramatic growth in power conversion energy (PCE), from about 3.7% in 2009<sup>10</sup> to over 25.8% in 2023.<sup>11</sup> Such incredible improvements in PCE can be attributed to a large number of modifications in layer deposition techniques,<sup>12–15</sup> the type of electron transport (ETLs)<sup>16–22</sup> and hole-transport materials (HTMs)<sup>23–29</sup> used, the use of efficient additives<sup>30</sup> and stabilizers,<sup>26,31–35</sup> different perovskite compositions, and so on.<sup>36–38</sup> In light of all of these, PSCs have attracted a high level of marketing activity by removing barriers to commercialization through the growth in PCE, increasing stability, environmental compatibility, and the possibility of scaling.<sup>38</sup> One very promising option for decreasing the cost of PSCs is modification of the HTM, which has the highest price amongst the materials used to fabricate PSCs.<sup>39–41</sup> For example, the total synthetic cost of 1 g of spiro-OMeTAD, hereafter designated as compound (3), as the most used HTM in efficient PSCs, is about \$92, which rises dramatically to about \$170–425 when brought to market.<sup>42–44</sup>

Such a high cost for (3) has resulted from certain drawbacks in its manufacture, including: (1) use of a large number of synthesis steps (five in total); (2) a huge number of rounds of purification, which leads to lowering of the volume of the

<sup>a</sup> Group for Molecular Engineering of Advanced Functional Materials (GMA)

Department of Chemistry, University of Zanjan, Zanjan, Iran.  
E-mail: shahroos@znu.ac.ir

<sup>b</sup> School of Aerospace Engineering, University of Rome "La Sapienza", Via Salaria, 851 – 00138 Rome, Italy

<sup>c</sup> Department of Electronics Engineering, University of Rome Tor Vergata, Via del Politecnico 1, 00133 Roma, Italy

<sup>d</sup> CHOSE – Centre for Hybrid and Organic Solar Energy, University of Rome "Tor Vergata", via del Politecnico 1, Rome 00133, Italy

† Electronic supplementary information (ESI) available. See DOI: <https://doi.org/10.1039/d3ya00367a>



product; and (3) use of expensive catalysts, such as dichloro[2,2'-bis(diphenylphosphino)-1,1'-binaphthyl]palladium(II).<sup>45,46</sup> Therefore, many attempts have been made to replace (3) with a low-cost HTM.<sup>46-48</sup> However, (3) also suffers significantly from low electrical conductivity, and needs to be doped with dopants such as lithium bis(trifluoromethanesulfonyl)imide and 4-*tert*-butylpyridine to increase its electrical performance.<sup>49</sup> However, by adding dopant to increase conductivity, the stability of PSCs based on (3) decreases. Hence, HTMs that are dopant-free are ideal candidates to replace (3).<sup>23,50,51</sup> With respect to this, here we try to address the dilemma of the presence of dopant and the stability<sup>52,53</sup> by using a dopant-free HTM. Thus, a very simple, cheap, and dopant-free HTM based on phenanthroimidazoles and having good stability is introduced.

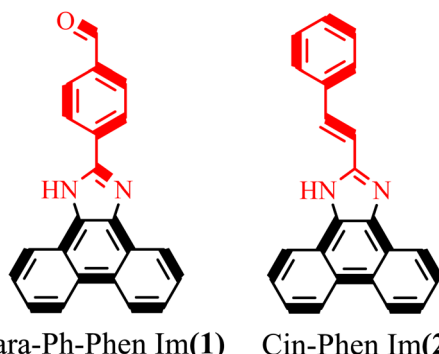
Surprisingly, the phenanthroimidazole family has some competence as a new building block for blue fluorescent materials<sup>54</sup> with high luminous efficiency,<sup>55</sup> a relative balance of carrier injection, efficient transport properties,<sup>56,57</sup> and excellent thermal stability.<sup>58</sup> In addition, phenanthroimidazoles show favourable properties, such as anti-inflammatory,<sup>59</sup> anti-lupus,<sup>60</sup> anticancer,<sup>61</sup> antibacterial,<sup>62</sup> antitumor,<sup>63</sup> and antiviral<sup>64</sup> activity. In addition, the application of phenanthroimidazoles as HTMs in PSCs has recently been reported.<sup>65-67</sup>

Phenanthroimidazole compounds combine the desirable properties of imidazole and phenanthrene as block cores. Phenanthroline enhances intermolecular  $\pi$ - $\pi$  packing and high cavity mobility, blocking the core with a planar  $\pi$ -bonded structure.<sup>68,69</sup> Five-membered heterocyclic imidazoles have two different nitrogen atoms, one with electron-poor character, as in pyridine, and one with electron-rich character, as in pyrrole.<sup>70,71</sup> A pyridine-like nitrogen atom as a Lewis base passivates perovskite defects. Furthermore, incorporation of the phenanthrene moiety improves the planarity of the imidazole-derived motif, thus promoting intermolecular  $\pi$ - $\pi$  stacking. Moreover, due to the different electronic properties of the two nitrogen atoms in the imidazole moiety, the hybrid phenanthroimidazole core exhibits low symmetry, especially after incorporating different donors, and side edges, which leads to less apparent symmetry throughout the molecule. This low-symmetry structure favours maintaining amorphous thin films with high morphological uniformity, and avoids crystallization.<sup>69,72</sup> Therefore, this hybrid core can provide not only high hole mobility and an interfacial passivation effect, but also excellent morphological uniformity of thin films.<sup>67</sup>

In view of all of these features, two very small HTMs based on phenanthroimidazole with different donors, with and without a carbonyl functional group and without using any dopant, were synthesized to investigate the effect of the presence of the carbonyl functional group and the reduction in cost and increase in stability of PSCs.

## 2. Results and discussion

Preparation of phenanthroimidazole derivatives was accomplished using a one-pot cyclizing reaction *via* a very simple



para-Ph-Phen Im(1) Cin-Phen Im(2)

Scheme 1 The molecular structure of the new hole-transport materials (HTMs).

route without the use of a catalyst or column chromatography purification.<sup>73-77</sup> The experimental details, including the methods and synthesis procedure for the HTMs, are presented in ESI,† S1 and S2. The molecular structures of the perovskite/HTMs are shown in Scheme 1. Synthesis reactions and molecular structures of the *para*-Ph-Phen Im, and Cin-Phen Im, which are designated as (1) and (2), are given in ESI,† Fig. S1. Moreover, all the spectroscopic and photovoltaic results obtained have been compared to benchmark values for the HTM spiro-OMeTAD, compound (3). The full characterizations, including Fourier-transform infrared spectroscopy, nuclear magnetic resonance, elemental analysis, and mass spectroscopy, are given in the ESI,† S1.

Generally, the phenanthroimidazole compounds containing a phenyl ring in the 2-position exhibit an absorption band at around 350 nm and a strong fluorescence band at about 438 nm.<sup>78-81</sup> Fig. 1(a) shows the normalized UV-vis absorption and photoluminescence (PL) spectra of two new HTMs and compares them with (3) as a benchmark HTM, in dimethylformamide (DMF) as solvent ( $1.0 \times 10^{-5}$  mol L<sup>-1</sup>). The absorption band at 300–400 nm is attributed to the intramolecular charge transfer of the  $\pi \rightarrow \pi^*$  transition, which agrees with earlier observations.<sup>82,83</sup> As shown in Fig. 1(a), (1) exhibits a 20 nm blueshift in comparison to (3), while (2) exhibits a slight shift to a longer wavelength, which is probably related to an extended  $\pi$ -conjugation effect.<sup>84</sup> Furthermore, the emission spectra of the HTMs in DMF solvent at room temperature were recorded and are shown in Fig. 1(a). All HTMs have a broad emission band in the range of 400–550 nm, which can be attributed to the  $\pi^* \rightarrow \pi$  transition.<sup>79,85</sup> The emission maxima of the HTMs are shifted to lower energies (showing a redshift of about 15 to 23 nm), with respect to (3). The electrochemical behaviour of (1), (2), and (3) was analysed by cyclic voltammetry in DMF solvent from 0.0 V to 2 V, using Ag/AgCl as a reference electrode (Fig. 1(b)). Generally, the phenanthroimidazoles exhibited two, and in some cases four, peaks in the anodic scan and no activity in the negative potential range.<sup>86</sup> As shown in Fig. 1(b), the onset oxidation potentials of (1) and (2) were observed at 0.57 and 0.65 V, respectively.<sup>87</sup> For (2), the first oxidation value is 0.05 V higher than (3), while in the case of (1) this value is 0.03 V lower than for (3), confirming that (1) is more easily



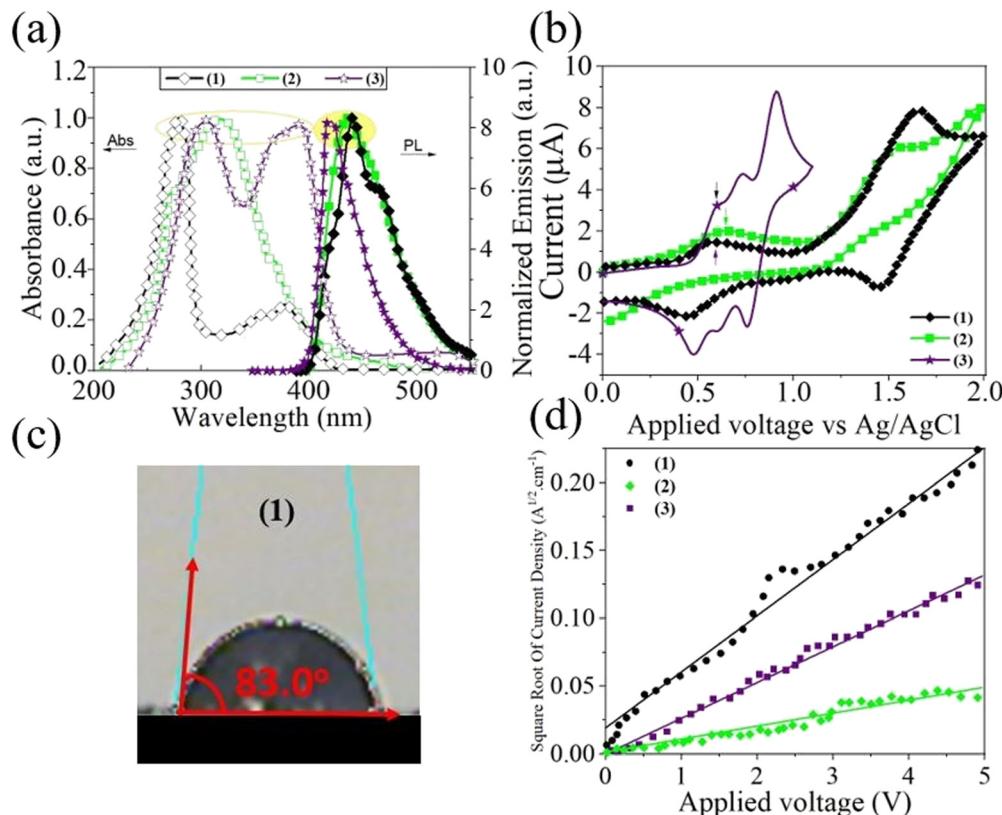


Fig. 1 (a) UV-vis and photoluminescence spectra of HTMs in DMF. (b) Cyclic voltammograms of HTMs and (3) as reference. (c) Contact angle of (1). (d) J-V characteristics of thin films in hole-conducting devices using HTMs with no doping (pristine state).

oxidized to  $(1)^+$  than  $(3)^+$  is to  $(3)^{+88}$ . Notably, a good energy balance between the highest occupied molecular orbital (HOMO) of the HTMs and the HOMO of the perovskite layer is a crucial feature to reach high efficiency PSCs.<sup>89,90</sup> The HOMO and LUMOs of the HTMs were calculated according to the equation,  $E_{\text{HOMO}} = -e(F_{\text{onset}}^{+} + 4.8)$  (eV), and  $E_{\text{LUMO}} = E_{\text{HOMO}} + E_{0-0}$ , which is summarized in Table 1.<sup>91,92</sup> Therefore, the HOMO energy levels were estimated to be  $-5.37$  and  $-5.4$  eV, and the LUMO levels  $-2.33$  and  $-2.34$  eV, respectively, for (1) and (2), which are in accordance with HOMO and LUMO energy levels of phenanthroimidazoles derivatives.<sup>93,94</sup> As mentioned above, these HOMO values are deeper than that of (3) ( $-5.21$  eV), which indicates their favourable level for hole extraction compared to (3), and with closer matching with the perovskite energy levels. This finding is promising for an efficient PSC based on the new HTMs because of the lower bandgap between the HOMO of the HTMs and the HOMO of the perovskite layer. By measuring the contact angle formed by

a water droplet under the (1) film surface, we can obtain more information on the surface energetics and wettability of the hole conductors. The water contact angles of (1) coated on glass was  $83.0^\circ$  (see Fig. 1(c)), which indicated its good hydrophobicity and suitability as an HTM in PSCs. Hence, the hydrophobic properties of (1) can efficiently prevent water penetration into the perovskite layer (ESI, † Fig. S2).

Important objectives for efficient dopant-free HTMs are the ability for charge carrier transport and for hole mobility.<sup>95</sup> As shown in Fig. 1(d), the space-charge-limited currents technique<sup>96–98</sup> was used to determine the hole mobility of the HTMs without using any dopant. Surprisingly, the estimated hole mobility value for (1), without the use of any additives, is about  $9.5 \times 10^{-4} \text{ cm}^2 \text{ V}^{-1} \text{ s}^{-1}$ , which is more than (3), with a value of about  $2.5 \times 10^{-5} \text{ cm}^2 \text{ V}^{-1} \text{ s}^{-1}$ . This means that the hole mobility of compound (1) is over 10 times that of (3) in the pristine sample.<sup>99–101</sup> Such high hole mobility and conductivity for the HTM (1) is very promising for an efficient dopant-free PSC. Fig. 2(a) shows the frontier orbital energy levels of (1), (2), and (3), as well as the components used in the fabrication of the PSC. Fig. 2(a) clearly reveals that the energy level of the HOMO of (1) ( $-5.37$  eV) is more closely matched with the perovskite energy level ( $-5.4$  eV) than for (3) ( $-5.21$  eV), resulting in (1) being more favourable than (3) for extracting holes from the perovskite layer to the HTM.

In fabricated PSCs, (1) and (2) were employed as new HTMs in an n-i-p structure in the configuration of FTO/compact  $\text{TiO}_2$

Table 1 Spectroscopic and electrochemical data for HTMs and (3)

HTM	$\lambda_{\text{abs}}$ (nm)	$\lambda_{\text{em}}$ (nm)	$E_{0-0}$ (eV)	$E_{\text{OX}}$ (V)	$E_{\text{HOMO}}$ (eV)	$E_{\text{LUMO}}$ (eV)	$\eta_{\text{quenching}}$
(1)	278, 355	440	3.03	0.57	-5.37	-2.33	0.92
(2)	270, 319	435	3.06	0.65	-5.4	-2.34	0.90
(3)	304, 378, 525 (sh)	421	3.04	0.6	-5.21	-2.17	0.96



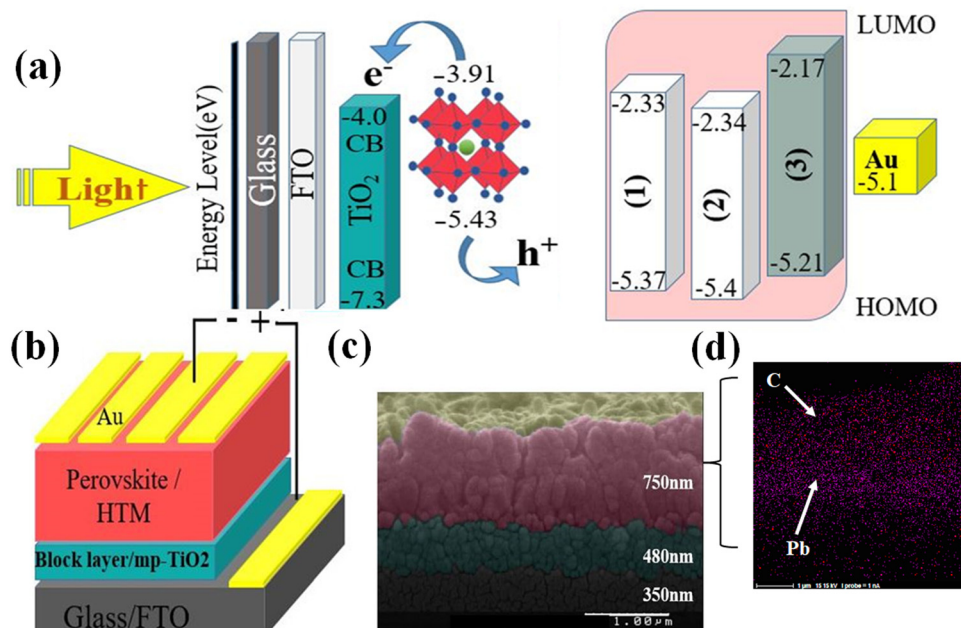


Fig. 2 (a) The relative energy levels in the two HTMs and (3). (b) Device architecture based on FTO/compact  $\text{TiO}_2$ /meso- $\text{TiO}_2$ /perovskite/HTMs/Au. (c) Cross-sectional map and (d) SEM image of PSC devices.

(~350 nm)/thin mesoporous  $\text{TiO}_2$  (~480 nm)/perovskite/HTM (~750 nm)/Au. A schematic of the device is shown in Fig. 2(b). The PSC device structures were kept exactly constant and just the HTMs were changed. This allows us to monitor the influence of the different HTMs. We also fabricated a PSC using (3) as the HTM as a reference. Fig. 2(c) shows a cross-sectional scanning electron microscopy (SEM) image of the arrangement of deposited layers of the constructed PSCs. As shown in the SEM image, the layers were successfully deposited and there are no defects or diffusion between layers.

The current density–voltage ( $J$ – $V$ ) curves for the new HTMs and the conventional HTM (3) are shown in Fig. 3, and the corresponding photovoltaic parameters are summarized in Table 2. The  $J$ – $V$  results indicated that using (1) for the HTM-based PSC showed a PCE of 14.06% with a  $V_{\text{OC}}$  of 1 V, a short-circuit current density ( $J_{\text{SC}}$ ) of  $19 \text{ mA cm}^{-2}$ , and a fill factor (FF) of 74%. This shows a higher efficiency compared to (2) and a slightly lower efficiency than (3) under the same device fabrication processes. Surprisingly, when dopants are removed from the HTMs, the photovoltaic parameters of (1) improved compared to (3). In fact, the dopant-free PSC based on (1) showed  $J_{\text{SC}}$ ,  $V_{\text{OC}}$ , FF, and PCE values of  $16.34 \text{ mA cm}^{-2}$ , 0.93 V, 0.69, and 9.11%, respectively, which are higher than for additive-free PSCs based on (3). The superior photovoltaic data for additive-free PSCs based on (1) can be attributed to the high mobility of (1), as discussed earlier.

The incident photon to current efficiency (IPCE) at short-circuit conditions as a function of wavelength, and integration of the IPCE spectra over the AM1.5G solar spectrum, provide the expected  $J_{\text{SC}}$  of the device under steady-state performance.<sup>102</sup> As can be seen in Fig. 3(b), the PSC made using (1) presented a higher quantum yield between 300 nm

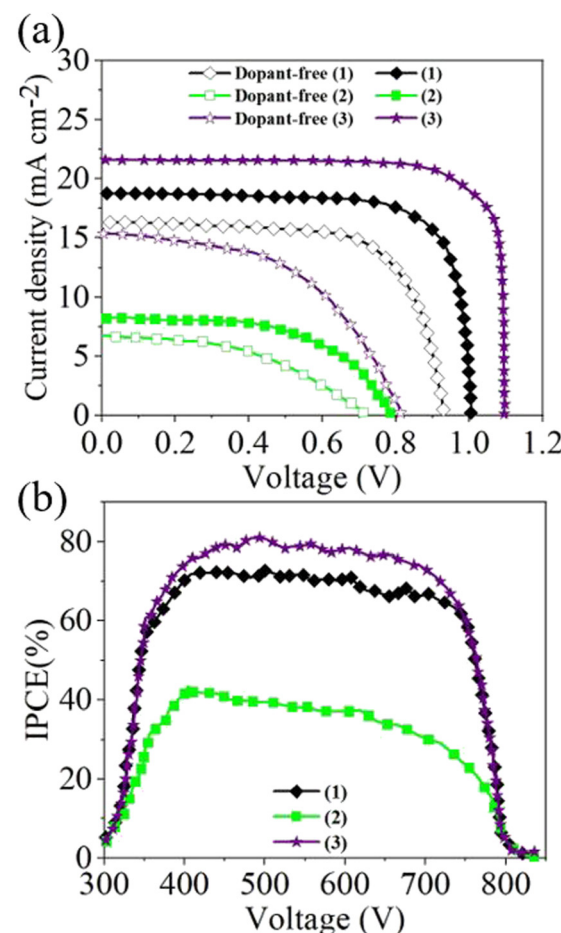


Fig. 3 (a)  $J$ – $V$  characteristics of PSCs based on the new HTMs containing dopant and free of dopant. (b) IPCE curves of the PSCs based on (1), (2) and (3).



**Table 2** The photovoltaic parameter of the perovskite based on various HTMs, (3)

HTM	$V_{OC}$ (V)	$J_{SC}$ (mA cm <sup>-2</sup> )	FF	PCE	Standard deviation (%)	Median (%)
(1)	1	19	74	14.06	2.05	11.62
Dopant-free (1)	0.93	16.34	60	9.11	0.99	7.12
(2)	0.8	8	55	3.52	0.45	2.55
Dopant-free (2)	0.72	6.71	45	2.17	0.46	0.94
(3)	1.1	22	77	18.63	1.2	16.01
Dopant-free (3)	0.81	15.34	50	6.21	0.74	4.45

and 850 nm than the PSC based on (2) and slightly lower than the benchmark PSC based on (3). The highest quantum yield reached was as high as 73% for (1), which agrees with the estimated  $J_{SC}$  value from the  $I$ - $V$  curve.

The statistical analysis of the photovoltaic performance of 15 PSCs based on (1), (2), and (3) is shown in Fig. 4. The standard deviation and median values of all parameters are given in Fig. 4 and in Table 2. Finally, the standard deviation and median values of the PCE of PSCs based on (1) are about 2.05% and 11.621%, which indicates the accuracy of results obtained.

A further promising finding is the high efficiency and stability of PSCs based on the new HTMs in the absence of any additives. We also compared the key role of additive on the efficiency and stability, as shown in Fig. 5. The PCE of (3) in the absence of additive dramatically decreased, while no large differences in PCE was observed for PSCs based on the new

HTMs, with and without additives. The encapsulation method and its details were as described in ref. 103.

As shown in Fig. 5(a), the PCEs of (1) and (3) are relatively similar, losing about 23% and 19% of their initial value, respectively, after 500 hours. In particular, the PCE of the additive-free PSC based on (1) showed less than 10% loss over 500 h. Finally, the dopant-free PSC based on (1) showed a PCE value of 9.11%, which is much more than the dopant-free PSC based on (3), with a PCE of 6.21%. The blueshift in the PL emission peak of the HTM coated on the perovskite can be attributed to the passivation process of the trap states close to the top surface of the perovskite, which dramatically decreases the stability and efficiency of PSCs.<sup>104</sup> These results clearly indicated that HTM (1) is very promising for dopant-free PSCs because of its high conductivity, which removes the need for the presence of co-conductive additives, such as LiTFSI/4-*tert*-butylpyridine.

The steady-state PL spectra of perovskite films on the new HTMs, (3), and pristine perovskite, as reference, were measured to compare the ability of the HTM for extracting photon-holes. The pristine perovskite film gives an emission band peak at approximately  $\approx 760$  nm, which is in accordance with the literature.<sup>32,91,99</sup> Clearly, strong PL quenching was achieved when the HTMs were coated on perovskite films, which suggested that (1) is a good quencher for perovskite films. Fig. 6(a) illustrates that perovskite/(3) and perovskite/(1) are more efficient than perovskite/(2), indicating their strong ability for extracting photo-holes from the perovskite active layer.

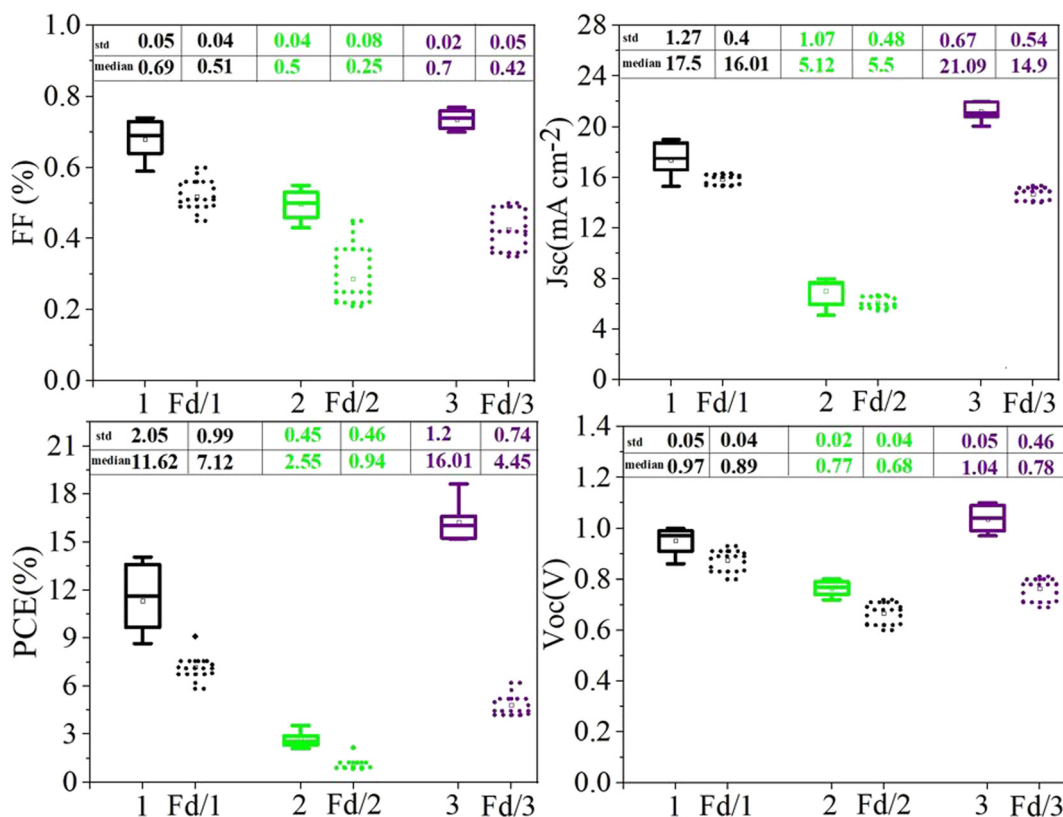


**Fig. 4** Statistical analysis of  $V_{OC}$ ,  $J_{SC}$ , FF, and PCE of PSCs based on (1), (2), and (3) in the presence and absence of additives. Fd = additive-free.



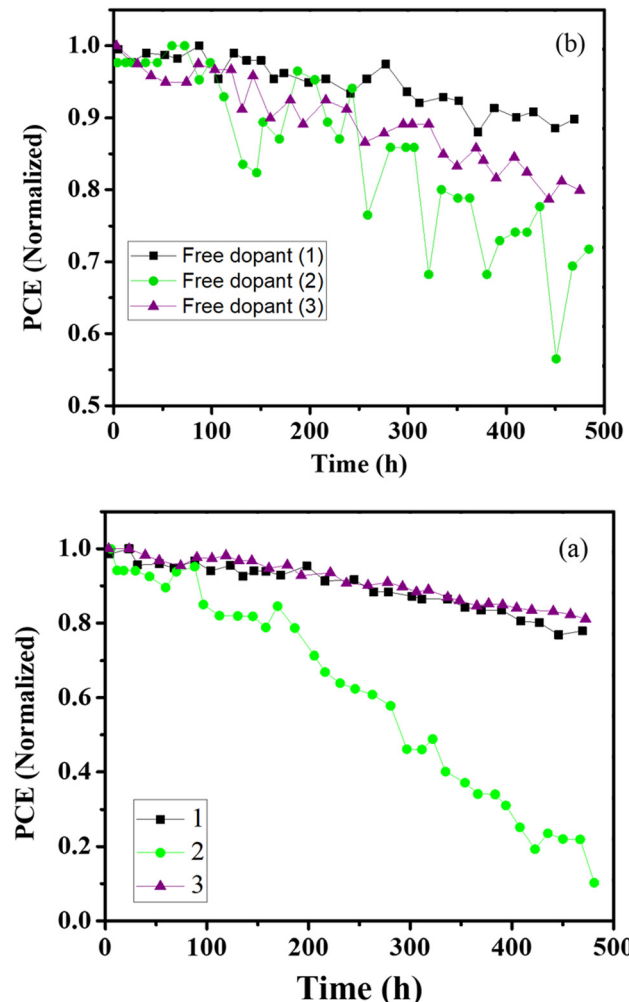


Fig. 5 (a) The stability of PSCs over time based on (1), (2), and (3) and (b) based on additive-free (1), (2), and (3).

PL quenching efficiency was calculated using the following formula:

$$\eta_{\text{quench}} = \frac{\text{PL}_{\text{bare}} - \text{PL}_{\text{quench}}}{\text{PL}_{\text{bare}}} \quad (1)$$

where  $\text{PL}_{\text{bare}}$  and  $\text{PL}_{\text{quench}}$  are the integrated PL intensities of perovskite on glass substrates without and with the quenching HTM layer.<sup>105</sup> The value of  $\eta_{\text{quenching}}$  for the HTMs is given in Table 1.

$\eta_{\text{quenching}}$  values for (1) and (3) were about 92% and 95%, respectively, which indicated that the (3)/perovskite film exhibited a slightly better PL quenching efficiency than (1)/perovskite. Interestingly, we proposed that the reason for the low efficiency of (2) is the unfavourable matching between the perovskite and the HTM. As shown in Fig. 6(a), the PL spectrum of perovskite film containing (2) shows a blueshift in wavelength, which can be attributed to the passivation of the trap states close to the top surface of the perovskite films.<sup>88,104</sup>

Time-resolved PL spectroscopy is a powerful technique to gain insight into the interface charge extraction behaviour and to estimate the photo-charge lifetime ( $\tau_2$ ) of perovskite and

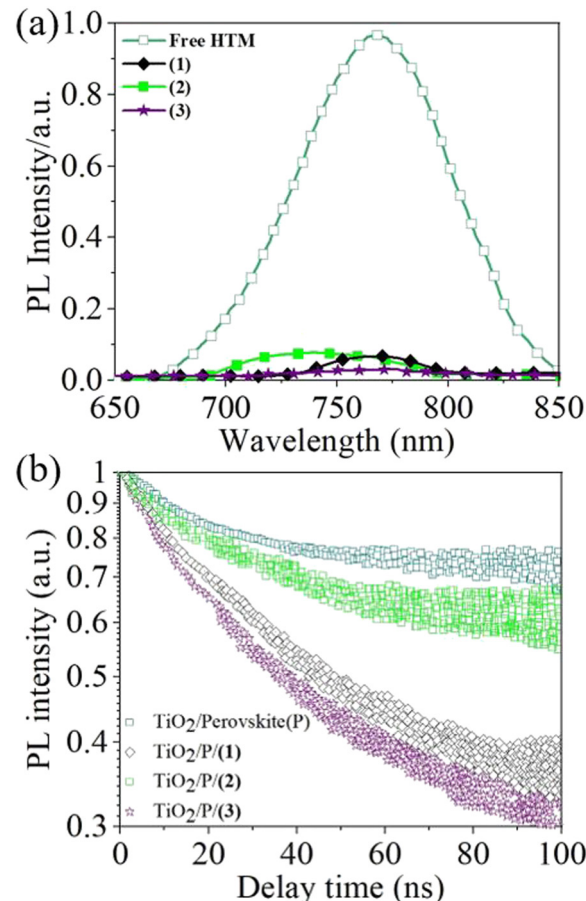


Fig. 6 (a) The steady-state PL spectra of glass/perovskite, glass/perovskite/(3), and glass/perovskite/doped HTMs. (b) The corresponding PL decay curves measured at a wavelength near the bandgap that yields a maximum PL signal upon exiting the perovskite,  $\text{TiO}_2/\text{perovskite/(3)}$ ,  $\text{TiO}_2/\text{perovskite/(1)}$ , and  $\text{TiO}_2/\text{perovskite/(2)}$  structures at 405 nm.

perovskite/HTM.<sup>106</sup> As shown in Fig. 6(b), the time-resolved PL decay patterns of  $\text{TiO}_2/\text{perovskite/(1)}$  and  $\text{TiO}_2/\text{perovskite/(3)}$  are relatively similar, with  $\tau_2$  of 8.5 ns and 7.7 ns, respectively, while the  $\tau_2$  of  $\text{TiO}_2/\text{perovskite}$  without HTM is about 16.9 ns.<sup>107</sup>

Fitting of the data obtained using bi-exponential functions indicated that the faster decay kinetics of (1) and (3) is due to the decreasing hole population generated close to the perovskite/HTM interface,<sup>108</sup> while the slower decay component of perovskite/(2) ( $\tau_2 = 15.2$  ns) could be associated with the holes created in the bulk of the perovskite, which can be proposed as a reasonable origin for the low efficiency of PSCs based on (2).

Both the high and fast PL quenching values indicate that (1) does act as an ideal hole acceptor, and hole transfer to the HTM is faster than diffusion out of the interface.

Thus, superior results are seen for the new HTMs with dramatically reduced cost compared to (3). Surprisingly, unlike (3), which requires a costly synthesis process with complicated sublimation steps for purification (it is synthesized in five reaction steps at a very low temperature ( $-78$  °C) and with high-cost Pd catalyst in an inert atmosphere conditions<sup>109,110</sup>), the new HTMs are synthesized in only one step and a simple



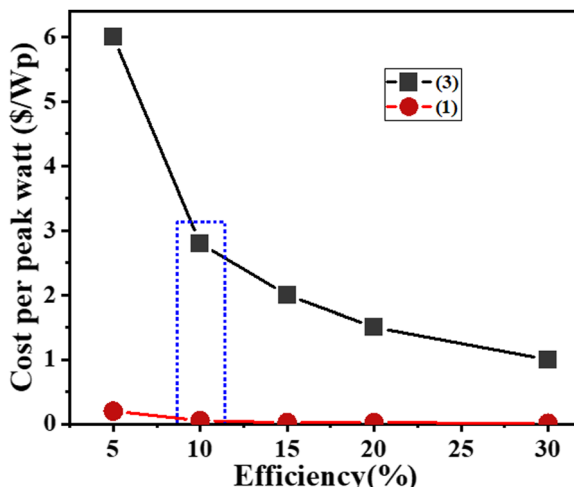


Fig. 7 Cost per peak watt (\$ per Wp) for (1) and spiro-OMeTAD (3).

low-cost process, without using any expensive Pd catalysts or other additives or column chromatography for purification.

The synthesis pathway of these compounds does not require expensive synthesis procedures. The synthetic details and estimated chemical costs of the synthesized HTMs were calculated according to the cost model described in ESI,† Table S1. It is noteworthy that the cost of (1) and (2) are approximately \$5.13 and \$5.18 per g, respectively, which is much cheaper than for (3) (\$92 per g).

Eqn (2) was used to further determine the cost per peak watt (\$\$ per Wp, denoted here as  $C_w$ ) for the utilization of the new HTM (1) and spiro-OMeTAD, where  $\eta$  is the solar cell efficiency in the range 5–30%,  $C_g$  is the cost-per-gram,  $p$  is the density which is assumed to be  $1.1 \text{ g cm}^{-3}$ ,  $t$  is the thickness of the donor material, and  $I$  is the solar insolation under peak conditions, which are assumed to be  $100 \text{ nm}$  and  $1000 \text{ W m}^{-2}$ , respectively.

$$C_w = \frac{(C_g \times p \times t)}{(\eta \times I)} \quad (2)$$

The plot of  $C_w$  as a function of solar cell efficiency reveals that the cost of preparation of HTM (1) is much more economical than for spiro-OMeTAD (Fig. 7). For example, for 10% efficiency, the cost of using the new HTM (1) is estimated to be \$0.056, whereas the estimated cost of using spiro-OMeTAD is \$3.003 for 10% efficiency. This means that the cost of HTM (1) is 0.02 times that of HTM (3).

Of note, the total cost and efficiency of the new HTMs was compared with 20 pioneer HTMs, and clearly showed the outstanding properties of new the HTMs in terms of both cost and efficiency amongst all HTMs reported so far in this group.

A comparison between the current work and other HTMs, in terms of synthesis costs and PCE, is shown in Fig. 8. The molecular structure of all HTMs, as well as the photovoltaic parameters, are given in ESI,† Table S2. The most important points in this comparison are related to the cost of preparation and the catalysts used during the reaction. As can be clearly seen, the lowest prices among all the HTMs belong to (1) and (2), at \$5.13 and \$5.18, respectively, which is much lower than for the other HTMs. In fact, the number of experimental steps

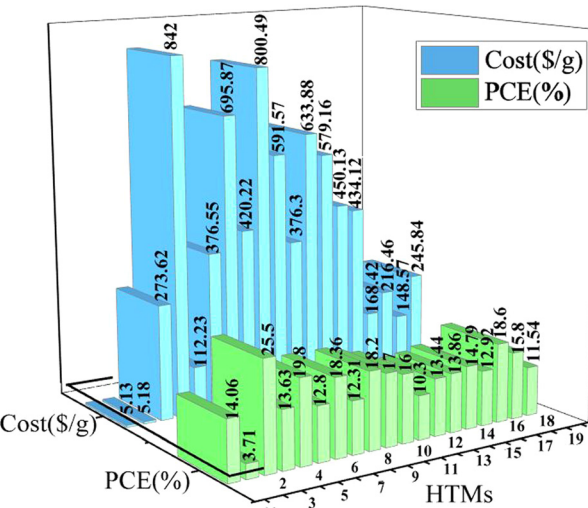


Fig. 8 Comparison between costs of organic HTMs (blue histograms) and the PCE of the corresponding PSCs (green histograms), as reported in our work and in other relevant literature. The HTMs reported in previous work are designated with numbers from 3 to 19. The molecular structure and photovoltaic data of all HTMs are given in the ESI,† Table S2.<sup>88,99,112–118</sup>

and use of catalyst causes this much bigger difference between the costs for the current HTMs *versus* the others.<sup>111</sup>

### 3. Conclusion

In summary, a facile and easy synthesis pathway for a small HTM for use in low-cost PSCs is presented. The reduction of the total cost of the benchmark (3) from \$100–400 per g to about \$5 per g for the newly synthesized HTM is very promising for large-scale production. Moreover, dopant-free PSCs based on HTM (1) showed good PCE ( $\approx 9.1$ ) along with remarkable stability over time (500 h), showing only a 10% loss of efficiency from the initial value. Moreover, the doped HTM also showed 14% efficiency and could retain more than 80% of its initial efficiency after 500 hours of light exposure. Additionally, the higher mobility of holes and greater conductivity of new HTM compared with (3) supported this photovoltaic performance. In particular, the PCE of the dopant-free PSC based on (1) is about two times that of (3) under the same conditions. In view of these results, one of the main aims of this paper is to encourage researchers to explore new avenues for the discovery of new, small HTMs that do not need support by a dopant for increasing conductivity, which should be of significant help in the future development and advancement of low-cost and high-stability PSCs for commercial applications.

### Author contributions

Sahar Majidi-Nezhad: methodology, investigation, formal analysis, and writing – original draft. Negin Sabahi: experimental analysis and writing – revision draft and editing. Hashem Shahroosvand: conceptualization, methodology, supervision,

resources, and writing – review and editing. Narges Yaghoobi Nia and Aldo Di Carlo: writing – review and editing.

## Conflicts of interest

The authors declare no conflict of interest.

## Acknowledgements

We deeply thank the University of Zanjan for financial support and NYN and ADC acknowledge the support of the Italian Ministry of Economic Development within the framework of the Operating Agreement with ENEA for Research on the Electric System.

## Notes and references

- 1 A. R. Gollakota and C.-M. Shu, *Gondwana Res.*, 2023, **114**, 93.
- 2 J.-P. Correa-Baena, M. Saliba, T. Buonassisi, M. Grätzel, A. Abate, W. Tress and A. Hagfeldt, *Science*, 2017, **358**, 739.
- 3 A. A. Brown, B. Damodaran, L. Jiang, J. N. Tey, S. H. Pu, N. Mathews and S. G. Mhaisalkar, *Adv. Energy Mater.*, 2020, **10**, 2001349.
- 4 N. Y. Nia, D. Saranin, A. L. Palma and A. Di Carlo, *Solar Cells and Light Management*, Elsevier, 2020, p. 163.
- 5 H. Zhou, Q. Chen, G. Li, S. Luo, T.-B. Song, H.-S. Duan, Z. Hong, J. You, Y. Liu and Y. Yang, *Science*, 2014, **345**, 542.
- 6 L. Yang, J. Feng, Z. Liu, Y. Duan, S. Zhan, S. Yang, K. He, Y. Li, Y. Zhou and N. Yuan, *Adv. Mater.*, 2022, **34**, 2201681.
- 7 S. Zhan, Y. Duan, Z. Liu, L. Yang, K. He, Y. Che, W. Zhao, Y. Han, S. Yang and G. Zhao, *Adv. Energy Mater.*, 2022, **12**, 2200867.
- 8 L. Fagioli and F. Bella, *Energy Environ. Sci.*, 2019, **12**, 3437.
- 9 J. W. Lee, D. K. Lee, D. N. Jeong and N. G. Park, *Adv. Funct. Mater.*, 2019, **29**, 1807047.
- 10 A. Kojima, K. Teshima, Y. Shirai and T. Miyasaka, *J. Am. Chem. Soc.*, 2009, **131**, 6050.
- 11 Y. Meng, C. Liu, R. Cao, J. Zhang, L. Xie, M. Yang, L. Xie, Y. Wang, X. Yin and C. Liu, *Adv. Funct. Mater.*, 2023, **33**, 2214788.
- 12 Y. Zhang, S.-W. Ng, X. Lu and Z. Zheng, *Chem. Rev.*, 2020, **120**, 2049.
- 13 P. Roy, N. K. Sinha, S. Tiwari and A. Khare, *Sol. Energy*, 2020, **198**, 665.
- 14 N. Y. Nia, F. Giordano, M. Zendehdel, L. Cinà, A. L. Palma, P. G. Medaglia, S. M. Zakeeruddin, M. Grätzel and A. Di Carlo, *Nano Energy*, 2020, **69**, 104441.
- 15 Y. Han, T. Zuo, K. He, L. Yang, S. Zhan, Z. Liu, Z. Ma, J. Xu, Y. Che and W. Zhao, *Mater. Today*, 2022, **61**, 54.
- 16 H. Wang, H. Li, W. Cai, P. Zhang, S. Cao, Z. Chen and Z. Zang, *Nanoscale*, 2020, **12**, 14369.
- 17 J.-F. Liao, W.-Q. Wu, Y. Jiang, J.-X. Zhong, L. Wang and D.-B. Kuang, *Chem. Soc. Rev.*, 2020, **49**, 354.
- 18 L. Gao and G. Yang, *Sol. RRL*, 2020, **4**, 1900200.
- 19 A. M. Elseman, C. Xu, Y. Yao, M. Elisabeth, L. Niu, L. Malavasi and Q. L. Song, *Sol. RRL*, 2020, **4**, 2000136.
- 20 G. Yang, H. Tao, P. Qin, W. Ke and G. Fang, *J. Mater. Chem. A*, 2016, **4**, 3970.
- 21 S. Navazani, N. Y. Nia, M. Zendehdel, A. Shokuhfar and A. Di Carlo, *Sol. Energy*, 2020, **206**, 181.
- 22 I. Ermanova, N. Yaghoobi Nia, E. Lamanna, E. Di Bartolomeo, E. Kolesnikov, L. Luchnikov and A. Di Carlo, *Energies*, 2021, **14**, 1751.
- 23 H. D. Pham, T. C. J. Yang, S. M. Jain, G. J. Wilson and P. Sonar, *Adv. Energy Mater.*, 2020, **10**, 1903326.
- 24 L. Calió, S. Kazim, M. Grätzel and S. Ahmad, *Angew. Chem., Int. Ed.*, 2016, **55**, 14522.
- 25 J. Urieta-Mora, I. García-Benito, A. Molina-Ontoria and N. Martín, *Chem. Soc. Rev.*, 2018, **47**, 8541.
- 26 N. Y. Nia, M. Zendehdel, M. Abdi-Jalebi, L. A. Castriotta, F. U. Kosasih, E. Lamanna, M. M. Abolhasani, Z. Zheng, Z. Andaji-Garmaroudi and K. Asadi, *Nano Energy*, 2021, **82**, 105685.
- 27 N. Y. Nia, F. Matteocci, L. Cina and A. Di Carlo, *ChemSusChem*, 2017, **10**, 3854.
- 28 N. Irannejad, N. Yaghoobi Nia, S. Adhami, E. Lamanna, B. Rezaei and A. Di Carlo, *Energies*, 2020, **13**, 2059.
- 29 N. Yaghoobi Nia, M. Bonomo, M. Zendehdel, E. Lamanna, M. M. Desoky, B. Paci, F. Zurlo, A. Generosi, C. Barolo and G. Viscardi, *ACS Sustainable Chem. Eng.*, 2021, **9**, 5061.
- 30 J. Chen and N. G. Park, *Adv. Mater.*, 2019, **31**, 1803019.
- 31 P. W. Liang, C. Y. Liao, C. C. Chueh, F. Zuo, S. T. Williams, X. K. Xin, J. Lin and A. K. Y. Jen, *Adv. Mater.*, 2014, **26**, 3748.
- 32 X. Li, M. Ibrahim Dar, C. Yi, J. Luo, M. Tschumi, S. M. Zakeeruddin, M. K. Nazeeruddin, H. Han and M. Grätzel, *Nat. Chem.*, 2015, **7**, 703.
- 33 L. Li, Y. Chen, Z. Liu, Q. Chen, X. Wang and H. Zhou, *Adv. Mater.*, 2016, **28**, 9862.
- 34 N. Yaghoobi Nia, E. Lamanna, M. Zendehdel, A. L. Palma, F. Zurlo, L. A. Castriotta and A. Di Carlo, *Small*, 2019, **15**, 1904399.
- 35 M. Vasilopoulou, A. Fakharuddin, A. G. Coutsolelos, P. Falaras, P. Argitis, A. R. bin Mohd Yusoff and M. K. Nazeeruddin, *Chem. Soc. Rev.*, 2020, **49**, 4496.
- 36 P. Schulz, D. Cahen and A. Kahn, *Chem. Rev.*, 2019, **119**, 3349.
- 37 C.-H. Chiang, M. K. Nazeeruddin, M. Grätzel and C.-G. Wu, *Energy Environ. Sci.*, 2017, **10**, 808.
- 38 M. Zendehdel, N. Y. Nia and M. Yaghoubinia, *Reliability and Ecological Aspects of Photovoltaic Modules*, IntechOpen, 2020, vol. 1, p. 93.
- 39 Y. Zhang, F. Wu, L. Chen, F. Zhang, Y. Ji, W. Shen, M. Li, Q. Guo, W. Su and R. He, *Sol. Energy Mater. Sol. Cells*, 2020, **212**, 110534.
- 40 Y. Cao, Y. Li, T. Morrissey, B. Lam, B. O. Patrick, D. J. Dvorak, Z. Xia, T. L. Kelly and C. P. Berlinguette, *Energy Environ. Sci.*, 2019, **12**, 3502.
- 41 L. Hajikhanmirzaei, H. Shahroosvand, B. Pashaei, G. Delle Monache, M. K. Nazeeruddin and M. Pilkington, *J. Mater. Chem. C*, 2020, **8**, 6221.



42 A. J. Huckaba, P. Sanghyun, G. Grancini, E. Bastola, C. K. Taek, L. Younghui, K. P. Bhandari, C. Ballif, R. J. Ellingson and M. K. Nazeeruddin, *ChemistrySelect*, 2016, **1**, 5316.

43 A. T. Murray, J. M. Frost, C. H. Hendon, C. D. Molloy, D. R. Carbery and A. Walsh, *Chem. Commun.*, 2015, **51**, 8935.

44 J. P. Wolfe and S. L. Buchwald, *J. Am. Chem. Soc.*, 1997, **119**, 6054.

45 J. P. Wolfe, H. Tomori, J. P. Sadighi, J. Yin and S. L. Buchwald, *J. Org. Chem.*, 2000, **65**, 1158.

46 P. Ruiz-Castillo and S. L. Buchwald, *Chem. Rev.*, 2016, **116**, 12564.

47 M. L. Petrus, K. Schutt, M. T. Sirtl, E. M. Hutter, A. C. Closs, J. M. Ball, J. C. Bijleveld, A. Petrozza, T. Bein and T. J. Dingemans, *Adv. Energy Mater.*, 2018, **8**, 1801605.

48 Š. Daškevičiūtė, N. Sakai, M. Franckevičius, M. Daškevičienė, A. Magomedov, V. Jankauskas, H. J. Snaith and V. Getautis, *Adv. Sci.*, 2018, **5**, 1700811.

49 S. Wang, Z. Huang, X. Wang, Y. Li, M. Günther, S. Valenzuela, P. Parikh, A. Cabreros, W. Xiong and Y. S. Meng, *J. Am. Chem. Soc.*, 2018, **140**, 16720.

50 L. Zhang, X. Zhou, C. Liu, X. Wang and B. Xu, *Small Methods*, 2020, **4**, 2000254.

51 T. Miyasaka, A. Kulkarni, G. M. Kim, S. Öz and A. K. Jena, *Adv. Energy Mater.*, 2020, **10**, 1902500.

52 G. Sathiyan, A. A. Syed, C. Chen, C. Wu, L. Tao, X. Ding, Y. Miao, G. Li, M. Cheng and L. Ding, *Nano Energy*, 2020, **72**, 104673.

53 J. Zou, J. Wu, W. Sun, M. Zhang, X. Wang, P. Yuan, Q. Zhu, J. Yin, X. Liu and Y. Yang, *Sol. Energy*, 2019, **194**, 321.

54 R. Sakamoto, N. Fukui, H. Maeda, R. Matsuoka, R. Toyoda and H. Nishihara, *Adv. Mater.*, 2019, **31**, 1804211.

55 S. Callaghan and M. O. Senge, *Photochem. Photobiol. Sci.*, 2018, **17**, 1490.

56 X. Ouyang, X.-L. Li, X. Zhang, A. Islam, Z. Ge and S.-J. Su, *Dyes Pigm.*, 2015, **122**, 264.

57 A. O. Eseola, O. Adepitinan, H. Görls and W. Plass, *New J. Chem.*, 2012, **36**, 891.

58 T. Jadhav, J. M. Choi, J. Shinde, J. Y. Lee and R. Misra, *J. Mater. Chem. C*, 2017, **5**, 6014.

59 N. G. Silva, R. O. Silva, S. R. Damasceno, N. S. Carvalho, R. S. Prudêncio, K. S. Aragão, M. A. Guimarães, S. A. Campos, L. M. Véras and M. Godejohann, *J. Nat. Prod.*, 2013, **76**, 1071.

60 I. Singh, V. Luxami and K. Paul, *Eur. J. Med. Chem.*, 2019, **180**, 546.

61 N. Rani, P. Kumar, R. Singh and A. Sharma, *Curr. Comput.-Aided Drug Des.*, 2015, **11**, 8.

62 N. Rani, A. Sharma and R. Singh, *Mini-Rev. Med. Chem.*, 2013, **13**, 1812.

63 I. Ali, M. N. Lone and H. Y. Aboul-Enein, *MedChemComm*, 2017, **8**, 1742.

64 B. Su, C. Cai, M. Deng and Q. Wang, *J. Agric. Food Chem.*, 2016, **64**, 2039.

65 M. Sheokand, Y. Rout and R. Misra, *J. Mater. Chem. C*, 2022, **10**, 6992.

66 S. A. Ok, B. Jo, S. Somasundaram, H. J. Woo, D. W. Lee, Z. Li, B.-G. Kim, J. H. Kim, Y. J. Song and T. K. Ahn, *Nat. Commun.*, 2018, **9**, 4537.

67 Y. Cheng, Q. Fu, X. Zong, Y. Dong, W. Zhang, Q. Wu, M. Liang, Z. Sun, Y. Liu and S. Xue, *Chem. Eng. J.*, 2021, **421**, 129823.

68 X. Zheng, Y. Hou, C. Bao, J. Yin, F. Yuan, Z. Huang, K. Song, J. Liu, J. Troughton and N. Gasparini, *Nat. Energy*, 2020, **5**, 131.

69 C. Shen, Y. Wu, H. Zhang, E. Li, W. Zhang, X. Xu, W. Wu, H. Tian and W. H. Zhu, *Angew. Chem., Int. Ed.*, 2019, **58**, 3784.

70 J. Wang, H. Zhang, B. Wu, Z. Wang, Z. Sun, S. Xue, Y. Wu, A. Hagfeldt and M. Liang, *Angew. Chem., Int. Ed.*, 2019, **131**, 15868.

71 F. Liu, F. Wu, W. Ling, Z. Tu, J. Zhang, Z. Wei, L. Zhu, Q. Li and Z. Li, *ACS Energy Lett.*, 2019, **4**, 2514.

72 B. Tu, Y. Wang, W. Chen, B. Liu, X. Feng, Y. Zhu, K. Yang, Z. Zhang, Y. Shi and X. Guo, *ACS Appl. Mater. Interfaces*, 2019, **11**, 48556.

73 A. Clarke, R. Anderson and B. Stone, *Phytochemistry*, 1979, **18**, 521.

74 A. Shienok, L. Kol'tsova, N. Zaichenko and V. Marevtsev, *Russ. Chem. Bull.*, 2002, **51**, 2050.

75 Y. Ooyama, H. Kumaoka, K. Uwada and K. Yoshida, *Tetrahedron*, 2009, **65**, 8336.

76 K. Skonieczny, J. Jaźwiński and D. T. Gryko, *Synthesis*, 2017, 4651.

77 N. L. Higuera, D. Peña-Solórzano and C. Ochoa-Puentes, *Synlett*, 2019, 225.

78 W.-C. Chen, Y. Yuan, Y. Xiong, A. L. Rogach, Q.-X. Tong and C.-S. Lee, *ACS Appl. Mater. Interfaces*, 2017, **9**, 26268.

79 W. Li, D. Liu, F. Shen, D. Ma, Z. Wang, T. Feng, Y. Xu, B. Yang and Y. Ma, *Adv. Funct. Mater.*, 2012, **22**, 2797.

80 R. Sarkar, T. Chaudhuri, A. Karmakar and C. Mukhopadhyay, *Org. Biomol. Chem.*, 2015, **13**, 11674.

81 K. Skonieczny, A. I. Ciuciu, E. M. Nichols, V. Hugues, M. Blanchard-Desce, L. Flamigni and D. T. Gryko, *J. Mater. Chem.*, 2012, **22**, 20649.

82 M. Daskeviciene, S. Paek, A. Magomedov, K. T. Cho, M. Saliba, A. Kizeleviciute, T. Malinauskas, A. Gruodis, V. Jankauskas and E. Kamarauskas, *J. Mater. Chem. C*, 2019, **7**, 2717.

83 F. Zhang, S. Wang, H. Zhu, X. Liu, H. Liu, X. Li, Y. Xiao, S. M. Zakeeruddin and M. Grätzel, *ACS Energy Lett.*, 2018, **3**, 1145.

84 R. Shang, Z. Zhou, H. Nishioka, H. Halim, S. Furukawa, I. Takei, N. Ninomiya and E. Nakamura, *J. Am. Chem. Soc.*, 2018, **140**, 5018.

85 V. Govindan, K.-C. Yang, Y.-S. Fu and C.-G. Wu, *New J. Chem.*, 2018, **42**, 7332.

86 R. Francke and R. D. Little, *J. Am. Chem. Soc.*, 2014, **136**, 427.

87 B. Rajamouli, R. Devi, A. Mohanty, V. Krishnan and S. Vaidyanathan, *New J. Chem.*, 2017, **41**, 9826.

88 K. Rakstys, A. Abate, M. I. Dar, P. Gao, V. Jankauskas, G. N. Jacopin, E. Kamarauskas, S. Kazim, S. Ahmad and M. Grätzel, *J. Am. Chem. Soc.*, 2015, **137**, 16172.



89 K. Rakstys, C. Igci and M. K. Nazeeruddin, *Chem. Sci.*, 2019, **10**, 6748.

90 L. Wang, J. Zhang, P. Liu, B. Xu, B. Zhang, H. Chen, A. K. Inge, Y. Li, H. Wang and Y.-B. Cheng, *Chem. Commun.*, 2018, **54**, 9571.

91 Y. Li, Y. Cao, J. Gao, D. Wang, G. Yu and A. J. Heeger, *Synth. Met.*, 1999, **99**, 243.

92 H. Zhu, F. Zhang, X. Liu, M. Sun, J. Han, J. You, S. Wang, Y. Xiao and X. Li, *Energy Technol.*, 2017, **5**, 1257.

93 M. Idris, C. Coburn, T. Fleetham, J. Milam-Guerrero, P. I. Djurovich, S. R. Forrest and M. E. Thompson, *Mater. Horiz.*, 2019, **6**, 1179.

94 D. Sylvinson MR, H.-F. Chen, L. M. Martin, P. J. Saris and M. E. Thompson, *ACS Appl. Mater. Interfaces*, 2019, **11**, 5276.

95 L. Bai, Z. Wang, Y. Han, Z. Zuo, B. Liu, M. Yu, H. Zhang, J. Lin, Y. Xia and C. Yin, *Nano Energy*, 2018, **46**, 241.

96 H. J. Snaith and M. Grätzel, *Appl. Phys. Lett.*, 2006, **89**, 262114.

97 T. Leijtens, I.-K. Ding, T. Giovenzana, J. T. Bloking, M. D. McGehee and A. Sellinger, *ACS Nano*, 2012, **6**, 1455.

98 B. Xu, E. Sheibani, P. Liu, J. Zhang, H. Tian, N. Vlachopoulos, G. Boschloo, L. Kloot, A. Hagfeldt and L. Sun, *Adv. Mater.*, 2014, **26**, 6629.

99 P. Ganesan, K. Fu, P. Gao, I. Raabe, K. Schenk, R. Scopelliti, J. Luo, L. H. Wong, M. Grätzel and M. K. Nazeeruddin, *Energy Environ. Sci.*, 2015, **8**, 1986.

100 A. Abate, S. Paek, F. Giordano, J.-P. Correa-Baena, M. Saliba, P. Gao, T. Matsui, J. Ko, S. M. Zakeeruddin and K. H. Dahmen, *Energy Environ. Sci.*, 2015, **8**, 2946.

101 Z. Hawash, L. K. Ono, S. R. Raga, M. V. Lee and Y. Qi, *Chem. Mater.*, 2015, **27**, 562.

102 J. A. Christians, J. S. Manser and P. V. Kamat, *J. Phys. Chem. Lett.*, 2015, **6**, 852.

103 J. Burschka, N. Pellet, S.-J. Moon, R. Humphry-Baker, P. Gao, M. K. Nazeeruddin and M. Grätzel, *Nature*, 2013, **499**, 316.

104 R. J. Westbrook, T. J. Macdonald, W. Xu, L. Lanzetta, J. M. Marin-Beloqui, T. M. Clarke and S. A. Haque, *J. Am. Chem. Soc.*, 2021, **143**, 12230.

105 B. Pashaei, H. Shahroosvand, M. Ameri, E. Mohajerani and M. K. Nazeeruddin, *J. Mater. Chem. A*, 2019, **7**, 21867.

106 N. Drigo, C. Roldan-Carmona, M. Franckevicius, K.-H. Lin, R. Gegevicius, H. Kim, P. A. Schouwink, A. A. Sutanto, S. Olthof and M. Sohail, *J. Am. Chem. Soc.*, 2019, **142**, 1792.

107 T. Leijtens, G. E. Eperon, A. J. Barker, G. Grancini, W. Zhang, J. M. Ball, A. R. S. Kandada, H. J. Snaith and A. Petrozza, *Energy Environ. Sci.*, 2016, **9**, 3472.

108 C. Motta, F. El-Mellouhi and S. Sanvito, *Sci. Rep.*, 2015, **5**, 1.

109 T. P. Saragi, T. Spehr, A. Siebert, T. Fuhrmann-Lieker and J. Salbeck, *Chem. Rev.*, 2007, **107**, 1011.

110 K. Rakstys, M. Saliba, P. Gao, P. Gratia, E. Kamarauskas, S. Paek, V. Jankauskas and M. K. Nazeeruddin, *Angew. Chem., Int. Ed.*, 2016, **128**, 7590.

111 B. Pashaei, S. Bellani, H. Shahroosvand and F. Bonaccorso, *Chem. Sci.*, 2020, **11**, 2429.

112 K. Rakstys, S. Paek, M. Sohail, P. Gao, K. T. Cho, P. Gratia, Y. Lee, K. H. Dahmen and M. K. Nazeeruddin, *J. Mater. Chem. A*, 2016, **4**, 18259.

113 H. Choi, K. Do, S. Park, J. S. Yu and J. Ko, *Chem. – Eur. J.*, 2015, **21**, 15919.

114 A. Molina-Ontoria, I. Zimmermann, I. Garcia-Benito, P. Gratia, C. Roldán-Carmona, S. Aghazada, M. Graetzel, M. K. Nazeeruddin and N. Martín, *Angew. Chem., Int. Ed.*, 2016, **55**, 6270.

115 M. Franckevičius, A. Mishra, F. Kreuzer, J. Luo, S. M. Zakeeruddin and M. Grätzel, *Mater. Horiz.*, 2015, **2**, 613.

116 S. Do Sung, M. S. Kang, I. T. Choi, H. M. Kim, H. Kim, M. Hong, H. K. Kim and W. I. Lee, *Chem. Commun.*, 2014, **50**, 14161.

117 P. Gratia, A. Magomedov, T. Malinauskas, M. Daskeviciene, A. Abate, S. Ahmad, M. Grätzel, V. Getautis and M. K. Nazeeruddin, *Angew. Chem., Int. Ed.*, 2015, **54**, 11409.

118 H. Choi, S. Paek, N. Lim, Y. H. Lee, M. K. Nazeeruddin and J. Ko, *Chem. – Eur. J.*, 2014, **20**, 10894.

